

RTG Student Lecture: Measurement of $|V_{ub}|$ at the LHCb experiment, lecture III

Michael Kolpin, Physikalisches Institut Heidelberg

May 9, 2016

In the first two lectures of this series we discussed how the magnitude of elements of the CKM matrix can be extracted by branching ratio measurements, and how these branching ratio measurements are in general performed at the LHCb experiment. Today we will be treating the specific measurement of $|V_{ub}|$ at LHCb, what additional complications occur, and how they are dealt with.

5 Measuring $|V_{ub}|$ with $\Lambda_b^0 \rightarrow p\mu\nu$ decays at LHCb

The baryonic decay mode $\Lambda_b^0 \rightarrow p\mu\nu$ was used for the first measurement of $|V_{ub}|$ at the LHCb experiment [1]. The main advantage of this decay mode is the comparably low amount of backgrounds containing real protons, faking the signal decay. Besides that, about every fifth b quark hadronises into a Λ_b^0 baryon (quark content u,d,b), allowing for a high statistical precision for processes with low branching ratios. Figure 1 shows a diagram depicting the decay.

One advantage of semileptonic decay modes is, as mentioned in lecture I, the fact that QCD interactions are limited to the hadronic part of the decay, encoded in so called form factors. However, due to the non-reconstructed neutrino, the yield extraction is much more complicated than for a fully reconstructed mode (as last week discussed for $B_{(s)}^0 \rightarrow \mu^+\mu^-$). The normalisation mode used in this analysis is $\Lambda_b^0 \rightarrow \Lambda_c^+(\rightarrow pK\pi)\mu\nu$, so the magnitude of $|V_{ub}|$ can be extracted from the relative branching ratio via

$$\frac{\mathcal{B}(\Lambda_b^0 \rightarrow p\mu\nu)}{\mathcal{B}(\Lambda_b^0 \rightarrow \Lambda_c^+\mu\nu)} = \frac{|V_{ub}|^2}{|V_{cb}|^2} \cdot R_{FF}, \quad (1)$$

where R_{FF} is the form factor ratio of both decays, given from theory calculations.

5.1 Partial reconstruction

The LHCb detector has both very precise vertex (due to the VeLo detector close to the beam pipe) as well as excellent momentum resolution. Using the flight direction information of the Λ_b^0 extracted from the vertex positions and comparing these to the

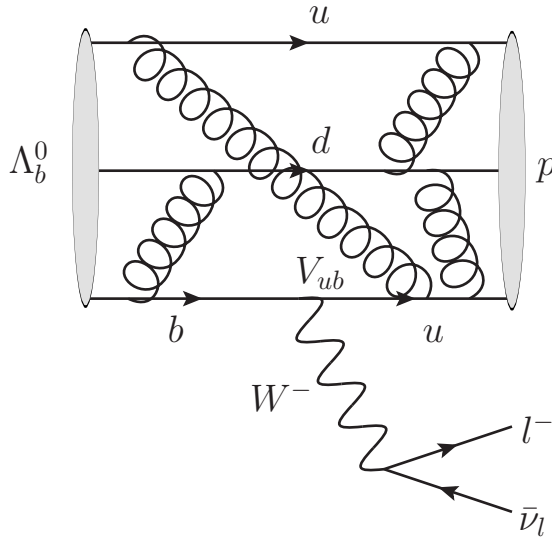


Figure 1: Diagram of the decay $\Lambda_b^0 \rightarrow p\mu\nu$.

momentum of the proton-muon system, the momentum missing perpendicular to the Λ_b^0 direction, p_\perp , can be derived. Figure 2 illustrates this procedure.

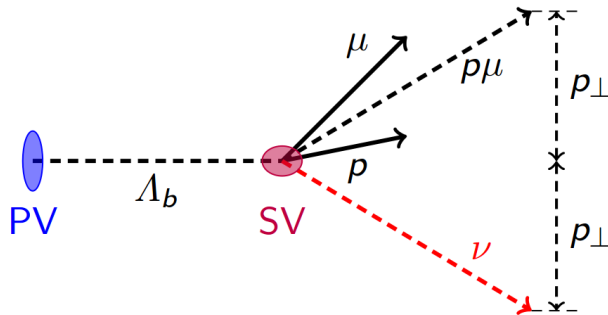


Figure 2: Partial reconstruction of p_\perp for $\Lambda_b^0 \rightarrow p\mu\nu$.

This p_\perp can be used to calculate the so-called "corrected mass" m_{corr} , defined as

$$m_{\text{corr}} = \sqrt{m_{\text{vis}}^2 + p_\perp^2} + p_\perp, \quad (2)$$

where m_{vis} is the mass of the visible, i.e. the proton-muon system. This construction is similar to the transversal mass variable used by e.g. the ATLAS experiment. Per construction m_{corr} peaks at the Λ_b^0 mass in case there is no mass missed in reconstruction (i.e. for a neutrino), and has generally lower values the more massive particles are not reconstructed. Figure 3 shows the corrected mass distributions for signal and normalisation

mode (which is also a background source) as seen in simulations, showing a clear separation in corrected mass. This separation increases further by requiring a low uncertainty of the corrected mass, which is chosen to be < 100 MeV.

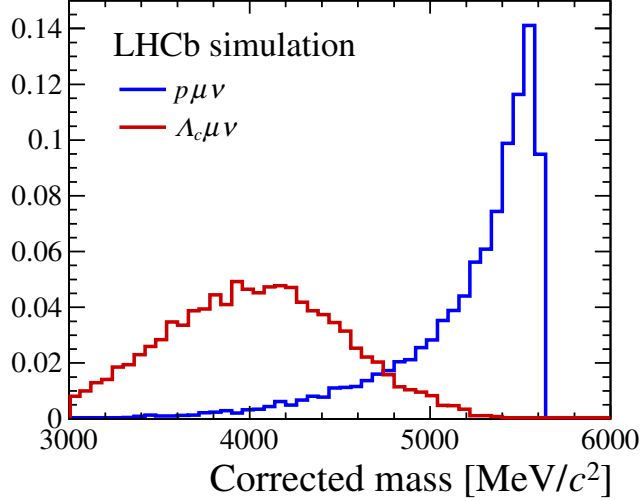


Figure 3: Corrected mass distributions for signal and normalisation modes.

In addition to reconstructing the corrected mass from vertex and momentum information, combining these with constraining the proton-muon-neutrino system to have the mass of the Λ_b^0 baryon, the momentum transfer $q^2 = (p_\mu + p_\nu)^2$ can be calculated. However, the calculation leads to a quadratic equation, thus leading to two possible solutions for most events.

5.2 Background treatment

The normalisation mode $\Lambda_b^0 \rightarrow \Lambda_c^+(\rightarrow pK\pi)\mu\nu$ used is at the same time the main background source. Due to $|V_{cb}| \sim 10 \cdot |V_{ub}|$, $b \rightarrow c$ transitions are about 100 times as likely as $b \rightarrow u$ transitions. And as even with the good separation shown in fig. 3, the background distribution has a long tail into the signal region, this large size difference makes it very hard to isolate a signal. Therefore, it is crucial to further reduce this background (and any kind of partial reconstructed backgrounds). For this, a so-called isolation BDT is used. This BDT uses information from multiple detector elements to check whether any additional charged tracks can be found, which are compatible with originating from the Λ_b^0 decay vertex. Figure 10 shows the BDT response for signal and background simulation. Applying this BDT removes 90% of the background while retaining more than 80% of signal events.

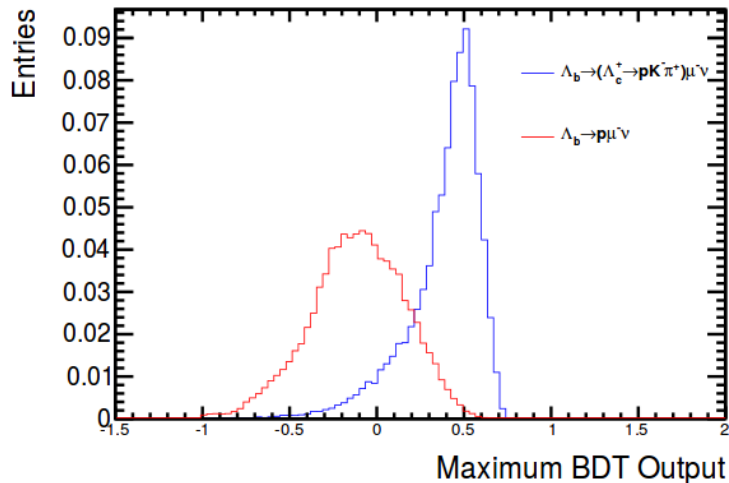


Figure 4: Isolation BDT response for signal and normalisation modes.

5.3 Minimising theory uncertainties

As mentioned earlier this lecture, to extract $|V_{ub}|$ from the measured relative branching fraction, we have to rely on form factor predictions (i.e. the required theory input). These predictions are using lattice QCD calculations [2], which have in general high uncertainties for lower q^2 values. Figure 5 shows the form factors and their uncertainties dependent on q^2 for both signal and normalisation mode. Thus, in order to not be completely dominated by theory uncertainties, signal (normalisation) events are required to have a q^2 values of $> 15 \text{ GeV}^2$ ($> 7 \text{ GeV}^2$). As there is a two-fold ambiguity in the q^2 calculation, this cut has to be applied to both solutions. These cuts have an efficiency of 38% (39%), but reduce the overall theory uncertainty affecting the final result to $\sim 5\%$.

5.4 Relative uncertainties

The relative uncertainties between signal and normalisation mode are mostly related to the different number of tracks in the final state (2 vs. 4), and differences in the respective simulation setup. Also the corrected mass error cut has a very different effect on signal and background. Figure 6 shows the different efficiencies (and corrections) and the final relative efficiency $\epsilon_{\text{sig}}/\epsilon_{\text{norm}} = 1.76 \pm 0.10$ (note the inverse definition to what we used before).

5.5 Result

The signal and normalisation yields are derived from fits to the corrected $p\mu$ and $pK\pi\mu$ masses, respectively. Figure 8 shows the results of both these fits. These are so-called template fits, where instead of an analytic function the signal and background shapes are

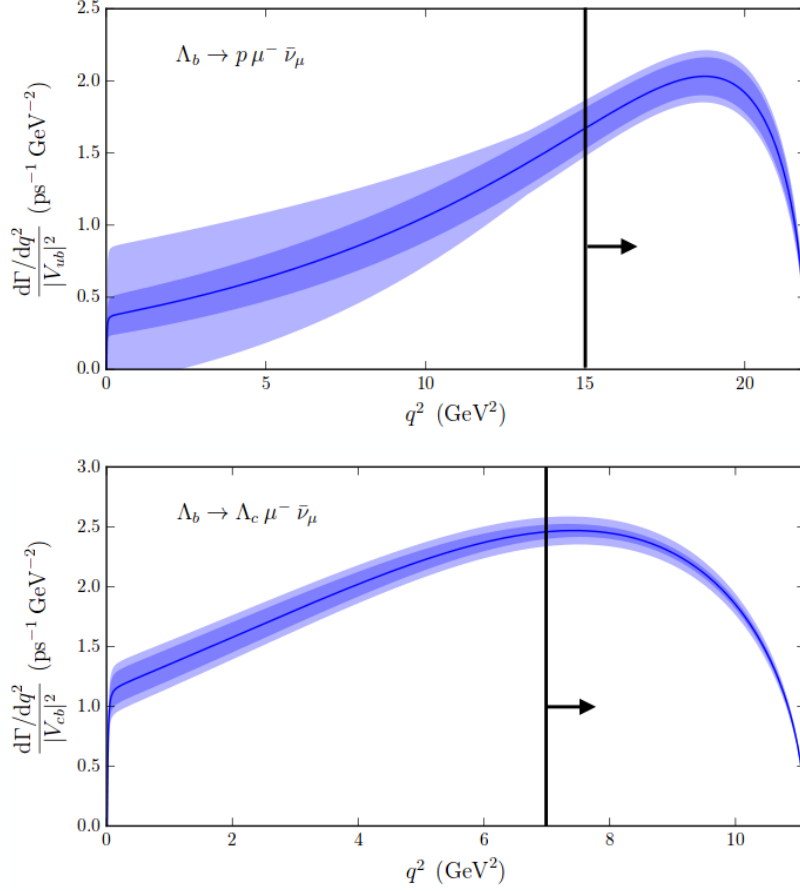


Figure 5: Form factors and uncertainties for signal and normalisation mode.

derived from simulation. These shapes are allowed to fluctuate within their respective uncertainties, to not be affected by the statistics of the respective simulation sample. The signal decay $\Lambda_b^0 \rightarrow p\mu\nu$ is clearly visible at the top end of the corrected mass spectrum. This is only possible due to the improved isolation techniques, and was never anticipated when the LHCb experiment started. The fit model in the $p\mu$ corrected mass contains many different decay modes, which can all be resolved reasonably well, while the $pK\pi\mu$ corrected mass spectrum is comparably simple and can be used to get a high precision on the normalisation yield.

Plugging all the measured values into our master formula

$$\frac{\mathcal{B}(\Lambda_b^0 \rightarrow p\mu\nu)}{\mathcal{B}(\Lambda_b^0 \rightarrow \Lambda_c^+ \mu\nu)} = \frac{N(\Lambda_b^0 \rightarrow p\mu\nu)}{N(\Lambda_b^0 \rightarrow \Lambda_c^+ (\rightarrow pK\pi)\mu\nu)} \cdot \mathcal{B}(\Lambda_c^+ \rightarrow pK\pi) \cdot \frac{\epsilon_{\text{norm.}}}{\epsilon_{\text{sig.}}}, \quad (3)$$

we derive the result

$$\frac{\mathcal{B}(\Lambda_b^0 \rightarrow p\mu\nu)|_{q^2 > 15 \text{ GeV}^2}}{\mathcal{B}(\Lambda_b^0 \rightarrow \Lambda_c^+ \mu\nu)|_{q^2 > 7 \text{ GeV}^2}} = (1.00 \pm 0.04(\text{stat.}) \pm 0.08(\text{sys.})) \cdot 10^{-2}. \quad (4)$$

Source	Relative efficiency
DecProdCut	0.645
Truth matching	1.04 ± 0.001
Stripping & Trigger	8.71
m_{corr} error	0.228
Isolation	1.049 ± 0.014
PID	1.173 ± 0.002
Tracking corr	0.995 ± 0.03
Trigger corr	1.032 ± 0.032
Λ_b^0 production	1.073 ± 0.005
Λ_c^+ decay model	0.998 ± 0.03
Λ_b^0 lifetime	1.042 ± 0.015
q^2 migration	0.95 ± 0.004
Form factor corr	0.985 ± 0.01
Total	1.76 ± 0.10

Figure 6: Relative efficiencies between signal and normalisation mode.

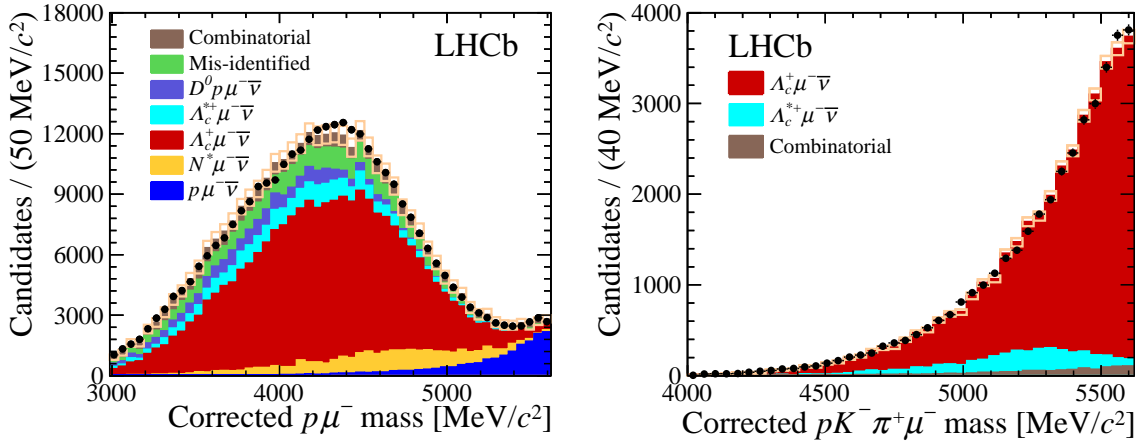


Figure 7: Corrected mass fits for signal and normalisation mode.

Using further $R_{FF} = 0.68 \pm 0.07$ [2] and $|V_{cb}| = (39.5 \pm 0.8) \cdot 10^{-3}$ [3], we can use formula 1 to calculate our final result of

$$|V_{ub}| = (3.27 \pm 0.15(\text{exp.}) \pm 0.16(\text{theo.}) \pm (0.06)(|V_{cb}|)). \quad (5)$$

This precision is on par with the previous world average, as reported by the PDG [3]. Figure ?? shows how this result compares to the inclusive and exclusive measurements, which we discussed in the first lecture: the LHCb agrees perfectly with other exclusive measurements, further increasing the tension between inclusive and exclusive measurements.

But how does this fit into the right-handed coupling hypothesis, which might give some

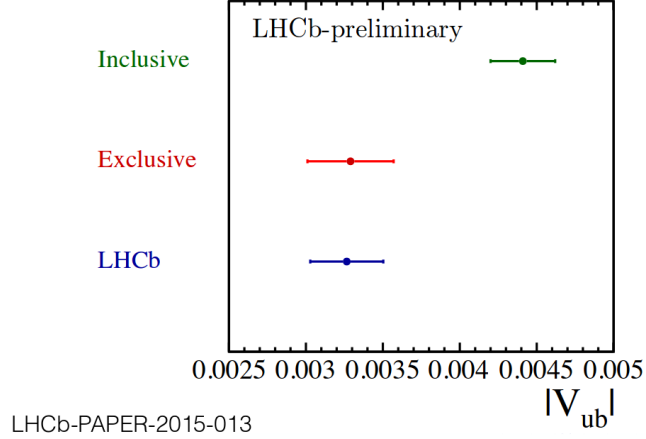


Figure 8: Comparison of $|V_{ub}|$ measurements.

hint to where the difference comes from? Figure 9 shows how the fit for the right-handed coefficient ϵ_R is affected by adding the new LHCb measurement. The discrepancy from the SM expectation ($\epsilon_R = 0$) is reduced, so no clear hint of such New Physics is found. Additional measurements are required to solve this puzzle.

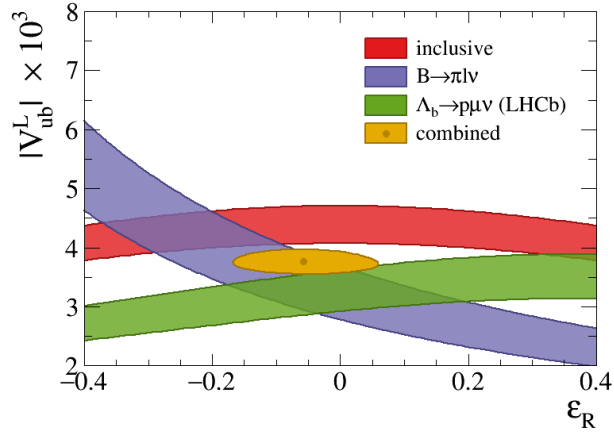


Figure 9: Updated fit for right-handed coupling coefficient [4].

6 Outlook: $|V_{ub}|$ from $B_s^0 \rightarrow K\mu\nu$

With the extremely precise result derived from Λ_b^0 baryon decays, interest has risen to improve this result by using other decay modes. While the "golden mode" $B^0 \rightarrow \pi\mu\nu$ is not feasible at a hadron collider due to the high pion background, the mode $B_s^0 \rightarrow K\mu\nu$ looks very promising. Table 1 shows the main differences between the kaon and Λ_b^0 modes: While the production rate for the kaon mode is slightly lower, it has the advantage of

Decay	$B_s^0 \rightarrow K^- \mu \nu$	$\Lambda_b^0 \rightarrow p \mu \nu$
Theory error	< 5%	5%
Prod. fract.	10%	20%
Branching ratio	$1 \cdot 10^{-4}?$	$4 \cdot 10^{-4}$
Charm \mathcal{B} error	$\pm 3.9\%$	+5.3%
Bkg. sources	$\Lambda_c^+, D_s^+, D^+, D^0$	Λ_c^+

Table 1: Comparison of K and Λ_b^0 modes.

having the potentially higher theoretical prediction and the more precise knowledge of the charm decay of the normalisation mode. However, there is much more background sources containing real kaon and muon pairs, being able to fake the signal decay.

Thus improved isolation criteria are important. For this analysis there is an even more advanced BDT being trained which adds also isolation against decays with additional neutral particles (e.g. $B_s^0 \rightarrow K^{*+}(\rightarrow K^+ \pi^0) \mu \nu$). Figure 10 shows the ROC curve (signal eff. vs. background rejection) of a very preliminary version of this BDT. Even in its early state, it is possible to remove more than 80% (50%) for backgrounds with additional charged (neutral) particles.

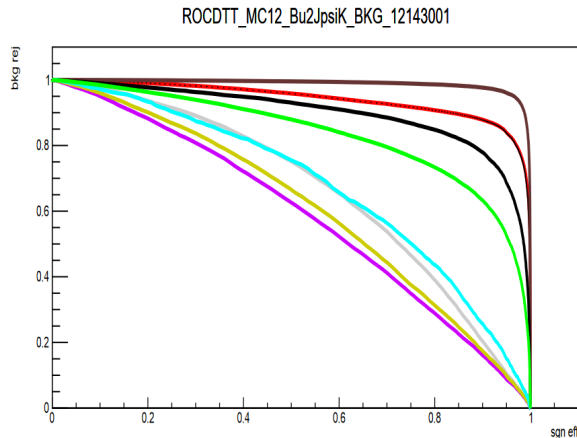


Figure 10: Preliminary ROC curve of charged and neutral isolation BDT.

Thus, the analysis of this decay mode looks very promising and progressing well, aiming for a publication this year.

References

- [1] LHCb collaboration, R. Aaij *et al.*, *Determination of the quark coupling strength $|V_{ub}|$ using baryonic decays*, Nature Physics **11** (2015) 743, arXiv:1504.01568.
- [2] W. Detmold, C. Lehner, and S. Meinel, *$b \rightarrow p\ell^-$ and $b \rightarrow \rho\ell^-$ form factors from lattice qcd with relativistic heavy quarks*, 1503.014211503.01421.
- [3] Particle Data Group, J. Beringer *et al.*, *Review of particle physics*, Phys. Rev. **D86** (2012) 010001, and 2013 partial update for the 2014 edition.
- [4] F. U. Bernlochner, Z. Ligeti, and S. Turczyk, *New ways to search for right-handed current in $b \rightarrow \rho \ell \nu$ decay*, 1408.25161408.2516.